

Supplementary Information

Organic flexible thermoelectric generators: from modeling, a roadmap towards applications

Davide Beretta^{1*}, Andrea Perego^{1,2}, Guglielmo Lanzani^{1,3}, Mario Caironi^{1**}

¹Center for Nano Science and Technology @PoliMi, Istituto Italiano di Tecnologia, via Pascoli 70/3, 20133 Milano (MI), Italy.

²Dipartimento di Energia, via Lambruschini 4, Politecnico di Milano, 20156 Milano (MI), Italy.

³Dipartimento di Fisica, P.zza Leonardo da Vinci 32, Politecnico di Milano, 20133 Milano (MI), Italy.

*E-mail: davide.beretta@iit.it

**E-mail of corresponding author: mario.caironi@iit.it

S1. Model approximations

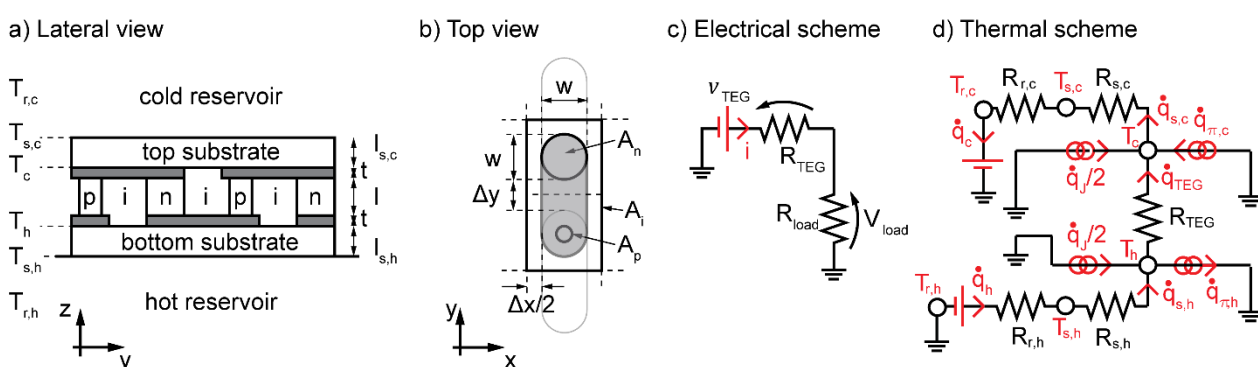


Figure 1. a) cross sectional lateral sketch of a typical device architecture. b) Top view of a thermocouple unit, made by a thermocouple and its insulation. c) Electrical scheme of the thermoelectric generator. R_{TEG} is the internal resistance of the generator, R_{load} the load resistance, V_{TEG} and V_{load} the voltage generated by the TEG and the voltage drop on load resistance respectively. d) Electrical equivalent of the thermal problem. In this scheme, the electrical resistances shown are representative of the thermal resistance (the inverse of the thermal conductance used in the model) of the various elements the model is made of, and the current represents the 1-D heat flux. Under stationary state hypothesis, the heat flux is conserved at each node. $R_{r,h}$ and $R_{r,c}$ are introduced in the model in order to take into account for the thermal resistances arising from the thermal coupling with the environment at the hot and cold side respectively.

The thermoelectric model used in this work is based on a series of approximations. These approximations are discussed one by one in the following subsections.

S1.1 Dimensionality of the model

The thermal and the electrical fluxes are 1-dimensional. This approximation is as good as smaller is the deviation of the temperature profile of the device from a 1-dimensional profile. Therefore, the accuracy of the model is as high (i) as smaller is the ratio between the lateral and the top surface of the device, (ii) as similar are the thermoelectric properties of the p- and n-type materials forming the thermocouples, and (iii) as thermally insulating is the electrical insulator used to separate the thermocouples legs, all of these aspects contributing to perturb the 1-dimensional temperature profile across the whole device.

S1.2 Constant thermoelectric parameters

The thermoelectric properties of the materials implemented in the models are constant within the temperature range spanned by the thermocouples under operating conditions. Since the model is for devices working under small temperature differences, and since no substantial variation of the thermoelectric properties of the materials considered is expected within small temperature intervals, the approximation does not influence significantly the accuracy of the model.

S1.3 Electrical resistance of the metallic interconnections

The electrical resistance of the metallic interconnections is neglected. This approximation is easily justified by evaluating the ratio between the resistance given by the metallic interconnections R_m and the resistance given by the thermocouples R_{pn} . In formula, the resistance of one thermocouple is

$$(1) \quad R_{pn} = \rho_p \frac{l}{A_p} + \rho_n \frac{l}{A_n} = \rho_{pn} \frac{l}{A_{pn}}$$

while the resistance of the metallic interconnections R_m can be estimated by geometrical considerations. In details, referring to Figure 1b,

$$(2) \quad R_m = \rho_m \frac{4w+2\Delta}{wt}$$

where $w^2 = \frac{4}{\pi} \max(A_p, A_n)$. Observing that $\Delta x = \Delta y = \Delta$, then $A_{pni} = (2w + 2\Delta)(w + \Delta)$ and the only acceptable value for Δ is $\Delta = -w + \sqrt{A_{pni}/2}$. Substituting, the resistance per unit area $r_m = R_m/A_{pni} = nR_m$ is found to be

$$(3) \quad r_m = n\rho_m \frac{2w+2\sqrt{A_{pni}/2}}{wt} = n\rho_m \frac{2}{t} + n\rho_m \frac{\sqrt{\pi A_{pni}}}{t\sqrt{2\max(A_p, A_n)}}$$

The contribution to the overall resistance given by the electrical interconnection is estimated by taking the ratio with respect to the resistance given by the thermocouples. At first order it follows

$$(4) \quad \frac{r_m}{nR_{pn}} \sim \frac{\rho_m}{\rho_{pn}} \frac{1/t}{l/A_{pn}} \left(1 + \frac{1}{\sqrt{FF}}\right)$$

Considering the typical resistivity of metals and highly doped conductive polymers, respectively in the order of $\sim 10^{-8} \Omega \text{ m}$ and $\sim 10^{-4} \Omega \text{ m}$, the contribution to the overall resistance given by the electrical interconnections is negligible only, and only if, $A_{pn}/l \ll 10^4 t$. Considering indicative values $A_{pn} \sim (100 \mu\text{m})^2$ and $l \sim 100 \mu\text{m}$, the conditions is satisfied for $t \gg 10 \text{ nm}$. In the models discussed, the condition is supposed to be always satisfied by an appropriate choice of the intermetallic connection thickness.

5.1.4 Electrical contact resistance

The electrical contact resistance due to the joining between dissimilar materials is neglected. The origin of the electrical contact resistance is mainly due to the soldering/joining mechanism, which determines band misalignment and more or less interdiffusion of different atomic species into the materials forming the joining. A dedicated experimental study to extract the electrical contact resistance is necessary for each couple of materials forming the joining. However, once known, it can be included as (temperature dependent) resistance series to the generator, such that neglecting this contribute doesn't lead, at first order, to any loss of generality in the modeling.

5.1.5 Thermal contact resistance

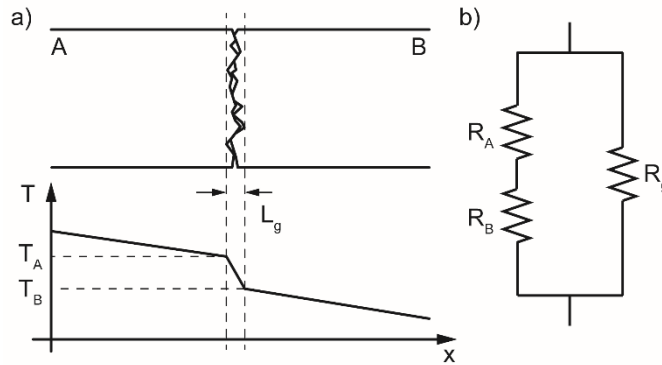


Figure 2. a) Thermal contact resistance between two dissimilar materials A and B, and their temperature profile. b) Equivalent electrical scheme of the thermal contact resistance.

The thermal contact resistance between dissimilar materials, i.e. a macroscopic effect due to the roughness of the joining surfaces that determines imperfect adhesion, and thus formation of voids, is neglected in the model. The approximation is justified by considering the contribution of the contact thermal resistance to the whole thermal resistance of the joining media. In particular, due to the typical processes involved in the fabrication of flexible TEGs and μ TEGs,¹⁻³ which involve printing methods, and/or photolithographic and physical vapor deposition techniques, all the interfaces, except the one between the substrates and the reservoirs, are supposed to be affected by a negligible contact thermal resistance. The case of the thermal contact resistance between a flexible substrate and the reservoir represents a special case in which, in general, a high and low thermally conductive media are joined.

Given a certain joining, depending on the matter filling the voids, the thermal contact conductance (namely the inverse of the thermal contact resistance) of the junction is more or less affected. According to J. P. Holman,⁴ and referring to Figure 2, the contact thermal

resistance can be modeled as the parallel of the thermal resistance of the voids with the thermal resistance series given by the two materials in direct contact. In formula

$$(5) \quad \dot{q} = \frac{1}{L_g} \left(2A_c \frac{\kappa_A \kappa_B}{\kappa_A + \kappa_B} + (A - A_c) \kappa_g \right) (T_A - T_B)$$

where $\frac{1}{AL_g} \left(A_c \frac{2\kappa_A \kappa_B}{\kappa_A + \kappa_B} + (A - A_c) \kappa_g \right) = h_c$ is the contact heat transfer coefficient, A the area of the joining, L_g the thickness of the contact, A_c the area of direct contact between the joining phases, $(A - A_c)$ the area left to the voids, κ_A , κ_B and κ_g the thermal conductivity of the joining media and of the filler respectively. Since A_c depends on many variables, such as surfaces roughness, materials elasticity and/or hardness, h_c is generally determined by experiments.⁵ Due to its importance in space and microelectronics, many analytical models in vacuum environment, where $\kappa_g = 0$, were derived.^{6,7} However, without entering into a detailed description, some conclusions can be stated by simple reasoning.

Let us consider for instance a case of joining between a high and a low thermally conductive media. Such joining could be the one between poly(ethylene 2,6-naphthalate) and aluminum, with thermal conductivity $0.15 \text{ W m}^{-1} \text{ K}^{-1}$ and $237 \text{ W m}^{-1} \text{ K}^{-1}$ respectively, where a thermally conductive paste with thermal conductivity $5 \text{ W m}^{-1} \text{ K}^{-1}$ is used. Considering a gap with thickness $1 \mu\text{m}$, then $h_c = 10^5 (0.3F + 5(1 - F))$, where $F = A_c/A$ is the surface fraction of direct contact joining. Therefore, depending on F , the heat transfer coefficient of the joining spans the interval $3 \cdot 10^5 < h_c < 5 \cdot 10^6 \text{ W m}^{-2} \text{ K}^{-1}$, which is much higher than the typical heat transfer coefficient of flexible substrates, and thus negligible in the model.

General considerations follow by considering the case $\kappa_A \ll \kappa_B$, such that the general expression of the thermal contact conductance h_c reduces to the much simpler expression

$$(6) \quad h_c \cong 2F \frac{\kappa_A}{L_g} + (1 - F) \frac{\kappa_g}{L_g}$$

Taking the ratio with respect to the thermal conductance of the substrate h_A , characterized by thermal conductivity κ_A and thickness L_A , it follows

$$(7) \quad \frac{h_c}{h_A} \cong 2F \frac{L_A}{L_g} + (1 - F) \frac{\kappa_g L_A}{\kappa_A L_g}$$

If $h_c/h_A \gg 1$ the thermal contact resistance is negligible with respect to the thermal resistance of the substrate and thus it can be discarded in the thermoelectric model. Depending on the filling material, choosing among pastes and epoxies allows the thermal conductivity of the gap to cover the interval $1 < \kappa_g < 10 \text{ W m}^{-1} \text{ K}^{-1}$. On the other hand, since flexible substrates, such as plastics or thin foils of Al_2O_3 , must be chosen in order to assure flexibility to the final thermoelectric device, κ_A falls in the range $0.1 < \kappa_A < 10 \text{ W m}^{-1} \text{ K}^{-1}$. Therefore, the ratio κ_g/κ_A is expected to span the range $0.1 < \frac{\kappa_g}{\kappa_A} < 100$. In Figure 3 the ratio $h_{\text{contact}}/h_{\text{sub}}$ versus the length ratio $L_{\text{sub}}/L_{\text{gap}}$ is shown, where h_{contact} and h_{sub} are the thermal conductance of the joining and of the substrate (namely the less conductive material forming the joining) respectively, L_{sub} and L_{gap} the thickness of the substrate and of the joining respectively. Different ratios $\kappa_{\text{gap}}/\kappa_{\text{sub}}$ are considered on the basis of the material properties discussed above, and the limit $F = 0$ and $F = 1$ are distinguished. In particular, the case $F = 0$ represents a very common condition where the gap filler is overdosed and the final joining presents a thin interlayer made of filler alone. This condition is preferable when $\kappa_{\text{gap}} > 2\kappa_{\text{sub}}$, while it is not recommended when $\kappa_{\text{gap}} < 2\kappa_{\text{sub}}$. By dosing the amount of filler, reducing the surface roughness of the materials forming the joining and/or exerting a certain mechanical pressure on the joining, the surface fraction of the joining left to voids can be tuned, thus allowing to match the condition $h_{\text{contact}}/h_{\text{sub}} \gg 1$. Considering plastic substrates characterized by thickness spanning the interval $10 - 100 \mu\text{m}$, and given $\kappa_{\text{gap}}/\kappa_{\text{sub}} = 10$, namely the typical case of plastic substrate ($\kappa_{\text{sub}} = 0.1$) and thermally conductive epoxy filler ($\kappa_{\text{gap}} = 1$), the thermal contact resistance is negligible for $L_{\text{gap}} < 1 - 10 \mu\text{m}$.

In the light of these considerations, the thermal contact resistance between the substrate and reservoirs in direct mechanical contact is always neglected in the model. Same considerations applies to the interfaces between substrates and heat exchangers in the case of air and liquid cooling: the thermal conductivity of typical materials used in the fabrication of the exchangers is much higher than the one of plastics, and thus, by a proper choice of thermally conductive adhesives, the thermal contact resistance among them is infinitesimal with respect to the one of the substrate.

5.1.6 Kapitza thermal resistance

The thermal boundary or Kapitza resistance, that is the resistance determined by the scattering of phonons at the interface between two dissimilar materials, is neglected. The Kapitza thermal resistances is due to the differences in their electronic and vibrational properties, and is thus present even at atomically perfect interfaces. In general, it is much smaller than the contact thermal resistance,

which was demonstrated to be negligible in the model, and is thus safely neglected. However, once known, it can be included as a (temperature dependent) resistance series term to the thermal resistance of the whole generator.

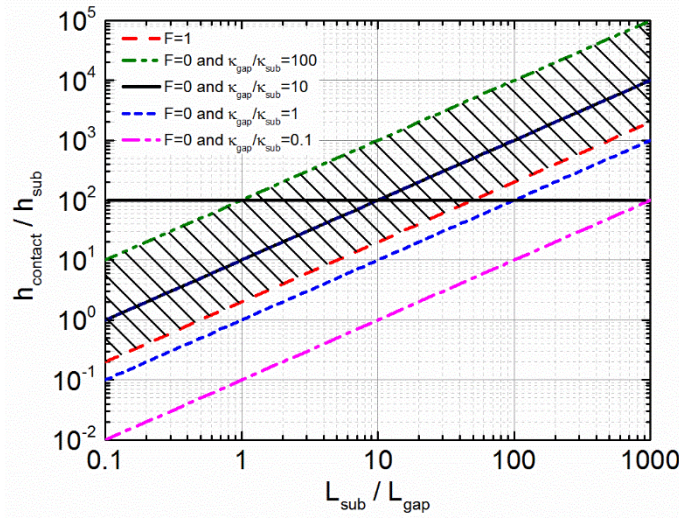


Figure 3. Thermal conductance ratio $h_{\text{contact}}/h_{\text{sub}}$ versus length ratio $L_{\text{sub}}/L_{\text{gap}}$ for different thermal conductivity ratio $\kappa_{\text{gap}}/\kappa_{\text{sub}}$ and surface fraction of direct contact joining F . Depending on the ratio $\kappa_{\text{gap}}/\kappa_{\text{sub}}$, $F = 0$, or $F = 1$ represents the best choice. The area of the graph patterned determines the range of $h_{\text{contact}}/h_{\text{sub}}$ achievable for $\kappa_{\text{gap}}/\kappa_{\text{sub}} = 100$ by spanning F from 0 to 1. It is the typical case of plastic substrate ($\kappa_{\text{sub}} = 0.1$) and thermally conductive epoxy filler ($\kappa_{\text{gap}} = 10$).

S2. Convective heat transfer coefficient

The convective heat transfer coefficients of different thermal coupling with the environment mechanisms are derived in the following. The cases of air and liquid cooling are considered. Please refer to S.1.5 for the case of thermal coupling by direct mechanical contact.

S2.1. Air cooling

The Reynolds, Prandtl and Grashof dimensionless numbers are here reported for clarity

$$(8) \quad Re_x = \frac{\rho v x}{\mu}$$

$$(9) \quad Pr = \frac{\mu C_p}{\kappa}$$

$$(10) \quad Gr_x = \frac{\beta g (T_{s,c} - T_{r,c}) x}{\rho}$$

where ρ is the density of air, v the relative velocity between the generator and the air, μ the dynamic viscosity of air, κ its thermal conductivity, C_p the specific heat of air, x the length of the exchanging surface considered, g the gravity, and β the coefficient of thermal expansion of air. The average heat transfer coefficient is expressed by

$$(11) \quad \overline{h_{r,c,x}} = \frac{\overline{Nu_x} \kappa_{\text{air}}}{x}$$

where $\overline{Nu_x}$ is the average Nusselt number, κ_{air} the thermal conductivity of air, and x the length of the exchanging surface.

Since the Nusselt number is a function of the geometry of the heat exchangers and of the flow regime, it has to be calculated case by case. In particular, four main cases are distinguished, namely the combination of natural and forced convection, with and without radiators:

- I. **No heat exchanger and natural convection.** From the Fishenden-Saunders relation,¹⁰

$$(12) \quad \overline{Nu_x} = C * Ra_x^n$$

where

$$(13) \quad C = 0.54 ; n = \frac{1}{4} \text{ if } Ra > 10^7$$

$$(14) \quad C = 0.14 ; n = \frac{1}{3} \text{ if } Ra < 10^7$$

and $Ra_x = Gr_x * Pr$ is the Rayleigh number, given by the product of the Grashof number with the Prandtl number.

II. **No heat exchangers and forced convection.** Depending on the flow regime, three subcases are distinguished,¹¹ namely:

a. Laminar flow along the whole flat surface

$$(15) \quad \overline{Nu}_x = 0.664 Re_x^{\frac{1}{2}} Pr^{\frac{1}{3}}$$

b. Turbulent flow along the whole surface

$$(16) \quad \overline{Nu}_x = 0.037 Re_x^{\frac{4}{5}} Pr^{\frac{1}{3}}$$

c. Transition flow at a certain length of the surface (corresponding to critical $Re_{cr} = 10^5$), which corresponds to a weighted average between laminar and turbulent flow:

$$(17) \quad A = 0.037 Re_{cr}^{\frac{4}{5}} - 0.664 Re_{cr}^{\frac{1}{2}}$$

$$(18) \quad \overline{Nu}_x = (0.037 Re_x^{\frac{4}{5}} - A) Pr^{\frac{1}{3}}$$

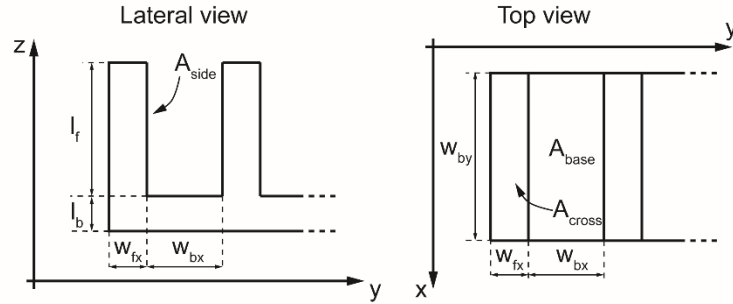


Figure 4. Schematic of the heat exchangers.

III. **Heat exchangers and natural convection.** Given the geometry of the exchangers shown in Figure 4, and under the hypothesis of adiabatic fin's tip (i.e. the tip of the fin does not exchange heat with the fluid, because of the small dimensions and the small temperature differences), the fin efficiency is defined as the ratio between the heat actually exchanged and the heat exchanged if the fin was isothermal at the temperature of the base¹¹:

$$(19) \quad \eta_{fin} = \frac{Q}{Q_{isothermal}} = \frac{\tanh(mL)}{mL}$$

where

$$(20) \quad m = \sqrt{\frac{h_{side} p}{\kappa_{exch} A_{cross}}}$$

is the fin parameter, A_{cross} the cross sectional area of the fin, p its perimeter and κ_{exch} the thermal conductivity of the material the heat exchanger is made of. Under these approximations, the Nusselt numbers are calculated for the vertical surfaces of the fin by

$$(21) \quad \overline{Nu}_L = \left[0.825 + \frac{Ra_L^{\frac{1}{4}}}{(1 + 0.49 Pr^{\frac{1}{4}})^{\frac{9}{8}}} \right]^2$$

where x stands for L , namely the vertical fins length (for the horizontal surfaces in natural convection, the coefficient is computed using the formulas discussed in A.1 section). Then, the heat transfer coefficient is calculated as the average of the heat transfer coefficients of the vertical and horizontal surfaces of the heat exchangers, that is

$$(22) \quad h_{rc} = \eta_{fin} \left[\left(h_{base} \frac{A_{base}}{A_{tot}} \right) + \left(h_{side} \frac{A_{side}}{A_{tot}} \right) \right]$$

IV. **Heat exchangers and forced convection.** The heat transfer coefficient is calculated as the average of the transfer coefficient of the vertical and horizontal surfaces, times the fin efficiency. In this case, h_{base} and h_{side} are calculated according to the relation already discussed for the case of forced convection and flat surface, distinguishing between the same three flow regimes.

The heat transfer coefficient for two different cases, namely $T_{r,c} = 302$ K and $T_{r,c} = 305$ K, are shown in Table 1. Since the typical area of the device we are referring to within this work is in the order of $\sim \text{cm}^2$, and since laminar to turbulent transition is unlikely to occur on such characteristics lengths, the flow regime is superimposed. To further investigate the influence of a mixed flow regime, a multidimensional model is required, which exceed from the purpose of this work.

Here, the two temperature drops considered are very close, and so are the average temperatures at which the thermophysical properties of the fluid are evaluated in the two cases. Therefore, since the heat transfer coefficients under forced convection depend on temperature only indirectly and by means of the thermophysical properties of the fluid, and since the thermophysical properties are slow functions of temperature, the coefficients of forced convection are found to be very similar. On the contrary, under natural convection the heat transfer coefficients directly depend on temperature, and differences among the two cases considered are appreciable.

In the case of fins array, further improvement could be made by increasing the base area of the dissipator and making it larger than the area of the device. In this work, for the sake of the calculations, coefficients are referred to the base area, without considering this possibility. However, by proper geometrical optimization, $h_{r,c}$ under natural convection can be significantly increased and made to fall in the order of $10^4 \text{ W m}^{-2} \text{ K}^{-1}$.

| $T_{r,c} = 302$ K | | | | |
|-------------------|---|-------------------|-------------------|---|
| | Forced Convection ($\text{W m}^{-2} \text{ K}^{-1}$) | | | Natural Convection ($\text{W m}^{-2} \text{ K}^{-1}$) |
| | Air Speed (m/s) | Laminar Regime | Turbulent Regime | |
| Flat surface | 10 | 12.319 | 37.84 | 1.6049 |
| | 50 | 27.54 | 137.12 | |
| Fins | 10 | $2.69 \cdot 10^3$ | $2.22 \cdot 10^3$ | 435.64 |
| | 50 | $4.66 \cdot 10^3$ | $5.34 \cdot 10^3$ | |

| $T_{r,c} = 305$ K | | | | |
|-------------------|---|-------------------|-------------------|---|
| | Forced Convection ($\text{W m}^{-2} \text{ K}^{-1}$) | | | Natural Convection ($\text{W m}^{-2} \text{ K}^{-1}$) |
| | Air Speed (m/s) | Laminar Regime | Turbulent Regime | |
| Flat surface | 10 | 12.318 | 37.84 | 2.0181 |
| | 50 | 27.54 | 137.12 | |
| Fins | 10 | $2.69 \cdot 10^3$ | $2.21 \cdot 10^3$ | 558.02 |
| | 50 | $4.65 \cdot 10^3$ | $5.33 \cdot 10^3$ | |

Table 1. Heat exchange coefficients for all the cases in air cooling, notice that for forced convection the values do not change significantly with a different reservoir temperature, since they are slow functions of the $T_{r,c}$.

S2.2 Liquid cooling

The liquid exchanger considered is composed by an array of parallel round tubes with diameter of 2 mm spaced by a gap of 2 mm. The hypothesis here is to consider fully developed flow, and this is true for tubes with $w/d > 10$, which is the case of the geometry considered.

We distinguish two flow regime with transition set for $\text{Re}_D = 10^4$, namely¹¹

- a. Laminar flow, with the boundary condition of constant surface temperature:

$$(23) \quad \overline{Nu_D} = 3.66$$

- b. Turbulent flow, using the Dittus-Boelter correlation:

$$(24) \quad \overline{Nu_D} = 0.023 * Re_D^{0.4} Pr^{0.4}$$

For these correlations, the reference dimension for Re and Nu is the hydraulic diameter of the tube, defined as:

$$(25) \quad D_H = \frac{4 * A}{P}$$

where A is the cross sectional area of the tube and P is the wetted perimeter. Data for different water mass flow are reported in Table 2.

| | Mass flow (ml/min) | $h_{r,c}$ (W m ⁻² K ⁻¹) |
|----------------|-----------------------|---|
| Liquid Cooling | 1 | 4.95 10 ³ |
| | 10 | 3.12 10 ⁴ |
| | 50 | 1.16 10 ⁵ |

Table 2. Convective heat transfer coefficients for liquid cooling, with respect to different water flows

Here the flow regime is always turbulent, due to the small diameter of the parallel tubes, which leads to higher coefficients, increasing with the mass flow.

Compared to air cooling, liquid exchangers are more efficient. As discussed in the previous section, further improvement could be made with more sophisticated geometries which require further and more complex calculations.

S.3 Radiative heat transfer coefficient

The contribution from radiation can be written as¹²

$$h_r^{rad} = \varepsilon \sigma_{SB} (T_r^2 + T_s^2) (T_r + T_s)$$

where ε is the surface emissivity and $\sigma_{SB} = 5.670373(21) \text{ W m}^{-2} \text{ K}^{-4}$ the Stefan-Boltzmann constant, such that multiplying it by $(T_r - T_s)$ the radiative thermal conductance fourth power law is recovered. ε is a dimensionless quantity spanning the interval 0 – 1, the typical value of common plastics being higher than 0.9. Generally, at low temperatures, the radiative heat transfer coefficient is very small with respect to the conductive and convective ones. For instance, $h_r^{rad} \sim 6\varepsilon \text{ W m}^{-2} \text{ K}^{-1}$ at room temperature and for $T_r - T_s = 5 \text{ K}$. Therefore, at low temperature and in almost all cases except natural convection from flat surfaces, where $h_r^{conv} \sim 1 \text{ W m}^{-2} \text{ K}^{-1}$, the radiative contribution to the whole heat transfer coefficient can be safely neglected.

S.4 Bibliography

- 1 G. J. Snyder, J. R. Lim, C.-K. Huang and J.-P. Fleurial, *Nat. Mater.*, 2003, **2**, 528–531.
- 2 W. Glatz, S. Muntwyler and C. Hierold, *Sensors Actuators A Phys.*, 2006, **132**, 337–345.
- 3 O. Bubnova, Z. U. Khan, A. Malti, S. Braun, M. Fahlman, M. Berggren and X. Crispin, *Nat. Mater.*, 2011, **10**, 429–433.
- 4 J. P. Holman, *Heat Transfer*, McGraw-Hill, 2010.
- 5 R. Kempers, P. Kolodner, A. Lyons and A. J. Robinson, *Rev. Sci. Instrum.*, 2009, **80**, 95111.
- 6 M. G. Cooper, B. B. Mikic and M. M. Yovanovich, *Int. J. Heat Mass Transf.*, 1969, **12**, 279–300.

- 7 M. M. Yovanovich, *IEEE Trans. Components Packag. Technol.*, 2005, **28**, 182–206.
- 8 S. R. de (Sybren R. Groot and P. (Peter) Mazur, *Non-equilibrium thermodynamics*, Dover Publications, 1984.
- 9 C. A. Domenicali, *Rev. Mod. Phys.*, 1954, **26**, 237.
- 10 M. W. Fishenden and O. A. Saunders, *An introduction to heat transfer*, 1950.
- 11 T. L. Bergman and F. P. Incropera, *Fundamentals of heat and mass transfer.*, Wiley, 2011.
- 12 G. Giambelli, *Lezioni di Fisica Tecnica. Parte Seconda. Trasmissione del Calore*, Tamburini Editore, Milano, 1971.